

## Sluggish $\sigma$ -Bond Formation between $sp$ -Hybridized Carbons: Acetylide Coupling on Ag(111)

Hsuan Kung,<sup>†</sup> Long-Cheng Lee,<sup>†</sup> Shin-Mou Wu,<sup>†</sup> Hsiu-Yao Cheng,<sup>‡</sup> and Chao-Ming Chiang<sup>\*,†</sup>

Department of Chemistry, Center for Nanoscience and Nanotechnology, National Sun Yat-Sen University, Kaohsiung, Taiwan 80424, and Department of Chemistry, Tunghai University, Taichung, Taiwan 40744

Received August 21, 2006; E-mail: cmc@mail.nsysu.edu.tw

Alkyne coupling reactions constitute powerful tools in various fields of chemistry, such as natural product, polymer, and supramolecular syntheses. To achieve linkage to  $sp$  carbon atoms, one of the most important strategies is the utilization of metal–acetylide reagents.<sup>1</sup> Knowledge about coupling reactions for chemisorbed acetylide groups on model metal surfaces has so far eluded the surface science literature.<sup>2</sup> Thus, current trend can only claim that  $C_{sp^2}-C_{sp^2}$  is slower than  $C_{sp^2}-C_{sp^3}$  coupling. For example, alkyl groups (ethyl or  $n$ -propyl) adsorbed on a Ag(111) surface, as measured by temperature programmed reaction (TPR), dimerize to higher alkanes below 210 K, while vinyl on the same surface recombines to butadiene at elevated temperatures ( $\sim 260$  K).<sup>3</sup> It is also curious that the ease of C–C reductive elimination from metal complexes exhibits an opposite propensity, where unsaturated hydrocarbon units eliminate faster than saturated alkyl groups.<sup>4</sup> Homocoupling of surface acetylides ( $M-C\equiv C-R$ ), creating a  $C_{sp}-C_{sp}$  connection, is worth investigating, and its added information should unravel if C–C  $\sigma$ -bond-forming rate and the hybridization state at the  $\alpha$ -carbon are related.

Silver surfaces are unique in their ability to couple hydrocarbon species without inducing dehydrogenation under vacuum.<sup>5</sup> To date, the isolation and identification of stable acetylide intermediates on a silver surface have only been accomplished by acetylene and propyne deprotonation on O/Ag(110).<sup>6,7</sup> Here we attempt to use propynyl iodide ( $I-C\equiv C-CH_3$ ) as precursor to generate  $Ag-C\equiv C-CH_3$  by facile C–I bond activation on Ag(111). Exposing Ag(111) to 5 Langmuirs (1 L =  $10^{-6}$  Torr·s)  $I-C\equiv C-CH_3$  ( $>97\%$ , TCI) at 110 K gave rise to a condensed multilayer reflection–absorption infrared spectrum (RAIRS) shown in Figure 1b, where all absorption features agree well with the major IR bands in Figure 1a taken from the liquid compound. The terminal  $CH_3$  group is evidenced by the stretching modes at 2956 (asymmetric,  $\nu_{as}$ ) and 2912  $cm^{-1}$  (symmetric,  $\nu_s$ ), as well as the deformation modes at 1430 ( $\delta_{as}$ ) and 1370  $cm^{-1}$  ( $\delta_s$ ). The band at 1022  $cm^{-1}$  is attributed to  $CH_3$  rock,  $\rho(CH_3)$ . The signature  $\nu(C\equiv C)$  mode appears at 2038  $cm^{-1}$ . Besides fundamentals, the remaining two weak bands at 2846 and 2190  $cm^{-1}$  are assigned to the asymmetric methyl deformation overtone,  $2\delta_{as}(CH_3)$ , and  $2\rho(CH_3)+\delta(C-I)$  combination,<sup>8</sup> respectively. Figure 1c displays vibration features originating from the monolayer species after the surface was annealed to 200 K. Here the vanished 2190  $cm^{-1}$  band reveals that the C–I bond is disrupted and  $I-C\equiv C-CH_3$  is converted into the desired  $Ag-C\equiv C-CH_3$ . The vibrations associated with dynamic dipole moments perpendicular to the CCC axis become relatively weak ( $\delta_{as}$  and  $\nu_{as}$ ) or even invisible ( $\rho$ ), whereas the intensities of those with opposite dipole direction either persist ( $\nu_s$  and  $\delta_s$ ), or grow, including the  $\nu(C\equiv C)$  and a new peak at 944  $cm^{-1}$  assigned to  $\nu(\equiv C-C)$ . These observations confirm that the surface-bound methylacetylide adopts a stand-up geometry (dipole selection rule) at this coverage. In fact, the tilt angle between

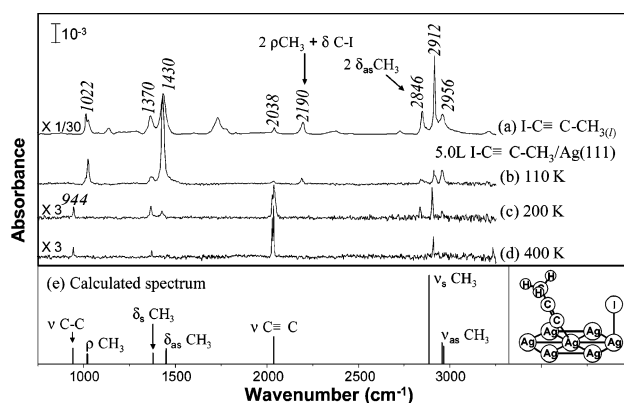


**Figure 1.** (a) IR spectrum of bulk sample in KBr. (b) RAIRS collected after a multilayer exposure of Ag(111) surface at 110 K to propynyl iodide. Spectra c and d were measured at 110 K following annealing of sample b to the temperatures indicated. All spectral features disappear above 400 K. Panel e is an IR spectrum with mode assignments based upon the animated vibrations of the calculated structure (inset). A recommended frequency scaling factor 0.9612 was used to correct systematic errors in the computation.<sup>11</sup>

the CCC axis and surface normal is estimated to be  $\sim 45^\circ$  by using the measured frequencies and band areas of the  $CH_3$   $\delta_s$  and  $\delta_{as}$  modes.<sup>9</sup> The frequency of the  $\nu(C\equiv C)$  exhibits no red-shift, so significant rehybridization does not occur upon formation of the  $Ag-C\equiv C-CH_3$ . It is likely that the acetylide moiety coordinates to the surface via a  $\sigma$ -metal–carbon bond with weak  $\pi$ -interactions. To substantiate our picture of bonding, we performed density functional theory (DFT) calculations at the B3LYP/LANL2DZ level using the Gaussian 03 program. The inset of Figure 1 represents the fully optimized structure,<sup>10</sup> and confidence in our recognition for the stable intermediate can be built on the good agreement between observed and calculated IR frequencies in Figure 1e.

TPR experiments were undertaken to verify if  $Ag-C\equiv C-CH_3$  underwent a C–C coupling reaction. As illustrated in Figure 2a, following 3.0 L  $I-C\equiv C-CH_3$  on Ag(111) at 200 K ( $\sim 50\%$  of monolayer saturation<sup>12</sup>), multiple-ion TPR indicates a desorption state characterized by concurrent  $m/z$  78 ( $C_6H_6^+$ ), 77 ( $C_6H_5^+$ ), 63 ( $C_5H_5^+$ ), 52 ( $C_4H_4^+$ ), 51 ( $C_4H_3^+$ ), and 50 ( $C_4H_2^+$ ) peaks with maxima ( $T_p$ ) at 490 K. The identity of the end-product was ratified as 2,4-hexadiyne ( $H_3C-C\equiv C-C\equiv C-CH_3$ ) by using the fragmentation patterns of NIST standards and consolidated by the same relative abundance of  $C_4$ ,  $C_5$ , and  $C_6$ -containing fragments in the TPR profiles measured after exposing Ag(111) to 2.0 L 2,4-hexadiyne ( $>98\%$ , TCI) at 110 K (shown in Figure 2b). The large temperature difference (490 vs 210 K) implicates that the diyne molecule resulting from  $Ag-C\equiv C-CH_3$  is not rate-limited by the final desorption step. The dimerization process follows second-order kinetics, testified by a TPR peak-shift toward lower temperatures as coverage increases from 0.5 to 7.0 L (shown in the inset

<sup>†</sup> National Sun Yat-Sen University.

<sup>‡</sup> Tunghai University.

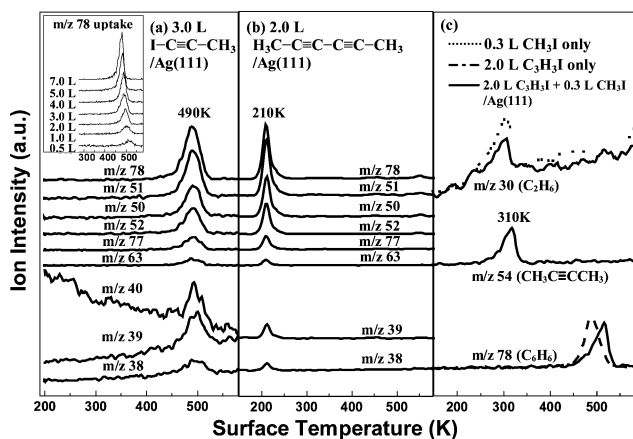


**Figure 2.** Multiplex TPR spectra from (a) propynyl iodide, (b) 2,4-hexadiyne, and (c) separate  $\text{CH}_3\text{I}$ ,  $\text{C}_3\text{H}_3\text{I}$ , and their mixture. Inset of panel a shows the  $\text{C}_6\text{H}_6$  product yield as a function of  $\text{C}_3\text{H}_3\text{I}$  exposure.

of Figure 2a). Also, the diffusion across the surface does not rationalize the slowness of the reaction, because the  $T_p$  remains high at large surface concentrations (diffusion is inhibited). It should be safe to argue that the  $\text{C}_{\text{sp}}-\text{C}_{\text{sp}}$  coupling step itself is rate-determining. Additional lower mass fragments, such as  $m/z$  2 ( $\text{H}_2$ ), 16 ( $\text{CH}_4$ ), 28 ( $\text{C}_2\text{H}_4$ ), and 30 ( $\text{C}_2\text{H}_6$ ), were surveyed but not found. However, a discernible desorption feature of  $m/z$  40 ( $\text{C}_3\text{H}_4^+$ ) at  $\sim 500$  K in Figure 2a indicates that  $\text{C}_3$  hydrogenated species were formed. The larger peak intensities of  $m/z$  39 and 38, compared to their normal contributions from hexadiyne, support propyne (or allene) liberation. Barteau et al. have found that  $\text{C}_3\text{H}_4$ , in fact, is the only hydrocarbon product (with no coupling) via methylacetylide disproportionation,  $4\text{C}_3\text{H}_3(\text{ad}) \rightarrow 3\text{C}_3\text{H}_4(\text{g}) + 3\text{C}(\text{ad})$ , at the same temperatures on  $\text{Ag}(110)$ .<sup>7</sup> Residual carbon was observed by XPS after heating the  $\text{C}_3\text{H}_3/\text{Ag}(111)$  to 800 K. Since  $\text{Ag}-\text{C}\equiv\text{C}-\text{CH}_3$  was generated from an iodo-compound instead of propyne deprotonation in this study, our discovery of the coupling product might correlate with the coadsorbed iodine, which was known for reducing the barrier for phenyl coupling on  $\text{Ag}(111)$ .<sup>13</sup> Perhaps an analogous promotion effect made the coupling route accessible and observable.

Concerning the coupling process, is it possible that the  $\text{C}_{\text{sp}}-\text{C}_{\text{sp}}$   $\sigma$ -bond is formed between the  $\beta$ -carbons in adjacent  $\text{Ag}-\text{C}\equiv\text{C}^\beta-\text{CH}_3$  (tail-to-tail dimerization)? This mechanism, reminiscent of the reverse diyne reaction with metallocene to give a bisacetylide complex,<sup>14</sup> invokes an unusual metalla-cyclocumulene intermediate. In Figure 1d, the spectrum taken after annealing  $\text{C}\equiv\text{C}-\text{CH}_3/\text{Ag}(111)$  to 400 K (near the onset of 2,4-hexadiyne evolution) shows no direct evidence for such reaction intermediacy. We are thus left with the alternative of head-to-head coupling between  $\alpha$ -carbons, which is conceptually straightforward, but the question is how the hybridization state of the  $\alpha$ -carbon influences the coupling rate. In light of the studies by Zhou and White,<sup>3</sup> the  $\sigma$ -bond formations of both  $\text{C}_{\text{sp}^3}-\text{C}_{\text{sp}^3}$  and  $\text{C}_{\text{sp}^2}-\text{C}_{\text{sp}^2}$  occur *below room temperature*. Yet our TPR data display that methylacetylide groups ( $\text{C}_{\text{sp}}$ ) couple at a temperature  $\sim 200$  K *higher* than vinyl groups ( $\text{C}_{\text{sp}^2}$ ), and  $\sim 250$  K *higher* than alkyl groups ( $\text{C}_{\text{sp}^3}$ ). These temperature differences translate into descending coupling rates in the order  $\text{sp}^3 > \text{sp}^2 \gg \text{sp}$ . We suggest two explanations in view of the metal-carbon ( $\text{M}-\text{C}$ ) bond breaking and  $\text{C}-\text{C}$  bond forming steps involved in the course of transformation. First, the  $\text{M}-\text{C}$  bond strengths generally follow the reverse order of  $\text{sp}^3 < \text{sp}^2 \ll \text{sp}$ , owing to the increased s-character in the carbon orbitals. So there exists a tie between the  $\text{C}-\text{C}$  coupling rate and the  $\text{M}-\text{C}$  bond strength, and the strongest  $\text{M}-\text{C}_{\text{sp}}$  bond renders the slowest  $\text{C}_{\text{sp}}-\text{C}_{\text{sp}}$  coupling. Second, Barteau and Madix have revealed that the  $\sigma$ -bonded acetylides on a silver

surface, like alkoxides, bear appreciable negative charge.<sup>15</sup> The anionic character bestowed on  $-\delta\text{C}\equiv\text{C}-\text{CH}_3/\text{Ag}$  is pronounced against vinyl or alkyl groups considering the high s-character in its  $\text{sp}$   $\alpha$ -carbon (electrons in s-orbital benefit from closer proximity to the nucleus). Anionic alkoxides can couple with relatively neutral alkyls quite easily on  $\text{Ag}(110)$ .<sup>16</sup> Similarly, TPR from a mixed-adlayer consisting of anionic  $\text{C}\equiv\text{C}-\text{CH}_3$  and  $\text{CH}_3$  led to a cross-coupled product, 2-butyne ( $m/z$  54), at a modest 310 K on  $\text{Ag}(111)$  in Figure 2c. It is conceivable that the energetic penalty for pairing up anionic  $-\delta\text{C}\equiv\text{C}-\text{CH}_3$  would be severe, albeit the increased s-character (more spherical and less directional) can facilitate the  $\alpha$ -carbon to adjust the  $\sigma$ -bonding orbital from the metal center toward each other.<sup>17</sup> On these bases, head-to-head coupling of the  $\text{sp}$ -hybridized carbons is highly hindered even in the presence of promoters (coadsorbed iodine atoms).

In conclusion, reactive acetylide intermediates have been generated and identified on a clean  $\text{Ag}(111)$  surface. The acetylide moieties self-couple at  $\sim 200$  K above room temperature, reflecting a much slower reaction rate against vinyl-vinyl or alkyl-alkyl coupling on the same surface. The  $\text{C}-\text{C}$  coupling rate appears to follow the order  $\text{C}_{\text{sp}^3} > \text{C}_{\text{sp}^2} \gg \text{C}_{\text{sp}}$ . The rate-determining step is reasonably ascribed to be a head-to-head dimerization involving bond construction between the  $\alpha$ -carbons. The relative  $\text{C}-\text{C}$  coupling rate is found to be sensitive to the hybridization state (s-character) in the  $\text{C}^\alpha$  orbital. Logical correlations between the coupling rate and the  $\text{M}-\text{C}$  bond strength as well as anionicity are established. The acetylide reactivity presented in our study would enrich the assortment of hydrocarbon chemistry discovered on single-crystal Ag surfaces.

**Acknowledgment.** We thank the financial support from the National Science Council of the Republic of China under Contract No. 94-2113-M-110-003. We are grateful to reviewers for their insightful comments.

**Supporting Information Available:** Calculated structures, energies, vibrational frequencies, and computational details. This material is available free of charge via the Internet at <http://pubs.acs.org>.

## References

- Marsden, J. A.; Haley, M. M. Cross-Coupling Reactions to sp Carbon Atoms. In *Metal-Catalyzed Cross-Coupling Reactions*; de Meijere, A., Diederich, F., Eds.; Wiley-VCH: Weinheim, Germany, 2004; pp 317–394.
- Ma, Z.; Zaera, F. *Surf. Sci. Rep.* **2006**, *61*, 229–281.
- Zhou, X.-L.; White, J. M. *J. Phys. Chem.* **1991**, *95*, 5575–5580.
- Collman, J. P.; Hegedus, L. S.; Norton, J. R.; Finke, R. G. *Principle and Applications of Organotransition Metal Chemistry*; University Science Books: Mill Valley, CA, 1987; pp 322–333.
- Zaera, F. *Chem. Rev.* **1995**, *95*, 2651–2693.
- Barteau, M. A.; Madix, R. J. *Surf. Sci.* **1982**, *115*, 355–381.
- Vohs, J. M.; Carney, D. A.; Barteau, M. A. *J. Am. Chem. Soc.* **1985**, *107*, 7841–7848.
- Nyquist, R. A. *Spectrochim. Acta* **1965**, *21*, 1245–1255.
- Fan, J.; Trenary, M. *Langmuir* **1994**, *10*, 3649–3657.
- The  $\text{Ag}(111)$  surface was modeled by a fixed  $\text{Ag}_7$  hexagonal cluster, where the acetylide group is bound to the center Ag atom. Adding an adjacent fixed iodine atom and an extra negative charge (making charge = -1 and multiplicity = 1) renders the most fitted IR spectrum.
- NIST Computational Chemistry Comparison and Benchmark DataBase, <http://srdata.nist.gov/cccbdb/vsf.asp>.
- A 6.0 L exposure corresponds to the monolayer saturation of  $\text{Ag}(111)$  with  $\text{I}-\text{C}\equiv\text{C}-\text{CH}_3$  at 200 K as determined by calibration TPR spectra that monitor the  $\text{C}_6\text{H}_6$  coupling product yield (shown in the inset of Figure 2a).
- Zhou, X.-L.; Schwane, A. L.; White, J. M. *J. Am. Chem. Soc.* **1993**, *115*, 4309–4317.
- Rosenthal, U.; Pellny, P.-M.; Kirchbauer, F. G.; Burlakov, V. V. *Acc. Chem. Res.* **2000**, *33*, 119–129.
- Barteau, M. A.; Madix, R. J. *Surf. Sci.* **1982**, *120*, 262–272.
- For example, see: Jones, G. S.; Barteau, M. A.; Vohs, J. M. *J. Phys. Chem. B* **1999**, *103*, 1144–1151.
- Low, J. J.; Goddard, W. A., III. *J. Am. Chem. Soc.* **1984**, *106*, 8321–8322.

JA066066X